Journal of Nuclear Science and Technology

ISSN: 0022-3131 (Print) 1881-1248 (Online) Journal homepage: https://www.tandfonline.com/loi/tnst20

A Current-Mode Detector for Unfolding X-ray Energy Distribution

Ikuo KANNO , Ryo IMAMURA , Kenta MIKAMI , Akio UESAKA , Makoto HASHIMOTO , Masahiko OHTAKA , Kuniaki ARA , Seiichiro NOMIYA & Hideaki ONABE

To cite this article: Ikuo KANNO , Ryo IMAMURA , Kenta MIKAMI , Akio UESAKA , Makoto HASHIMOTO , Masahiko OHTAKA , Kuniaki ARA , Seiichiro NOMIYA & Hideaki ONABE (2008) A Current-Mode Detector for Unfolding X-ray Energy Distribution, Journal of Nuclear Science and Technology, 45:11, 1165-1170, DOI: 10.1080/18811248.2008.9711905

To link to this article: https://doi.org/10.1080/18811248.2008.9711905

Published online: 05 Jan 2012.

Journal of NUCLEAR SCIENCE and TECHNOLOGY, Vol. 45, No. 11, p. 1165–1170 (2008)

ARTICLE

A Current-Mode Detector for Unfolding X-ray Energy Distribution

Ikuo KANNO[1,*], Ryo IMAMURA[1], Kenta MIKAMI[1], Akio UESAKA[1], Makoto HASHIMOTO[2], Masahiko OHTAKA[2], Kuniaki ARA[2], Seiichiro NOMIYA[3] and Hideaki ONABE[3]

[1]*Graduate School of Engineering, Kyoto University, Sakyo, Kyoto 606-8501, Japan*
[2]*Japan Atomic Energy Agency, O-arai, Ibaraki 311-1393, Japan*
[3]*Raytech Corporation, Yoto, Utsunomiya, Tochigi 321-0904, Japan*

(Received May 17, 2008 and accepted in revised form July 15, 2008)

To turn the advantage of energy measurement in x-ray transmission diagnosis into practice, we propose a novel detector for the estimation of x-ray energy distribution. This detector consists of several segment detectors arrayed in the direction of x-ray incidence. Each segment detector measures x-rays as current. With unfolding measured currents, the x-ray energy distribution is obtained. The practical application of this detector was verified by estimating the iodine thickness in an acryl phantom.

KEYWORDS: x-ray, energy distribution, transmission measurement, contrast media, unfolding, energy subtraction

I. Introduction

Reducing the exposure dose during x-ray transmission and computed tomography (CT) measurements is critical for the application of radiation detection techniques to the medical field. Previously, we proposed a filtered x-ray energy subtraction (FIX-ES) method in which the energy of an individual x-ray was measured for the detection of iodine contrast media;[1,2)] in conventional x-ray diagnosis, x-rays are measured as electrical current. The x-ray events in two energy ranges, which were lower and upper energies of the K-edge of the iodine contrast media, were employed as energy subtraction (ES) data. This FIX-ES method was twice as sensitive to the iodine as the conventional current measurement method.[3)] By optimizing the element and thickness of the filter material, the exposure dose could be reduced to 30% of that when white x-rays were employed. Moreover, the ES method gave CT values that were proportional to the thickness of the iodine contrast media, independent of the x-ray tube voltage or the size of the subject being tested.[4)] These data suggest that the CT taken by the ES method is immune to the beam hardening effect, which has a significant impact on the current measurement method.

However, the time required for energy measurement of x-rays is too long for practical use in medical CT measurements; the limitation of the counting rate in energy measurement does not allow the quick exposure required in practical diagnosis. As a solution to this problem, in the present study, we propose a novel detector that gives the energy distribution of incident x-rays when measuring them as current. We call this detector "transXend", as the x-rays transfix segment detectors, and the measured currents are transformed into x-ray energy distribution. The principle of the transXend detector is introduced first, followed by simple experiments and analysis of x-ray energy distribution measured using the transXend detector made of CsI(Tl) scintillators and photodiodes.

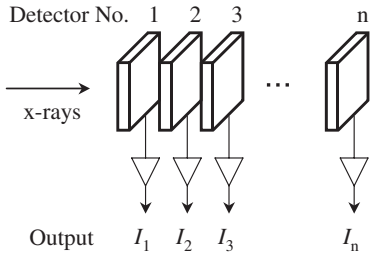

Fig. 1 Schematic drawing of the transXend detector

II. TransXend Detector

1. Operation Principle

The basic concept of the transXend detector involved utilizing the x-ray absorption coefficient of the detector substrate. As shown in **Fig. 1**, segment detectors are placed in the direction of the x-ray incidence. Each segment detector absorbs x-rays according to the energy of the x-ray and the absorption coefficient of the substrate. The energy of the absorbed x-ray is then turned into an electrical signal and is measured as a current. The x-rays with low energy tend to be absorbed in the forward segment detectors such as detectors 1 and 2. A part of the high-energy x-rays penetrates the forward segment detectors and is absorbed by the backward segment detectors. From the response function of each

*Corresponding author, E-mail: kanno@nucleng.kyoto-u.ac.jp

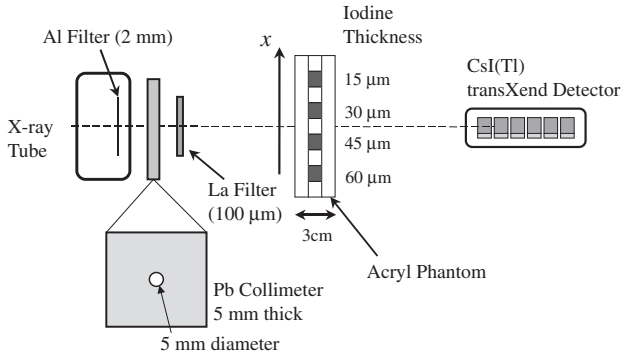

Fig. 2 Experimental setup for iodine thickness measurements with the transXend detector

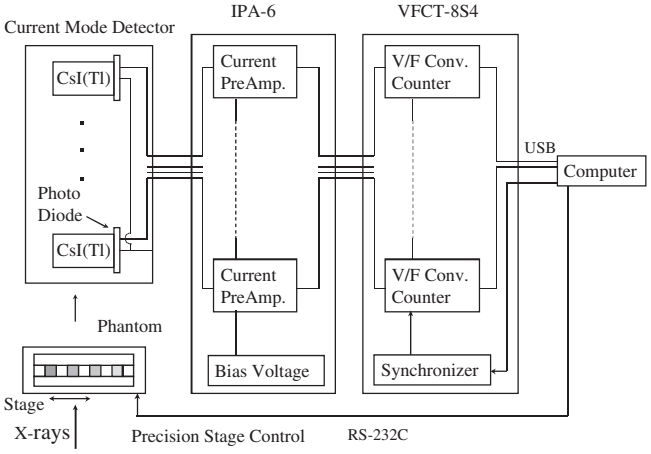

Fig. 3 Block diagram of the electronic circuit for the transXend detector (V/F Conv.: voltage-frequency converter)

segment detector, the energy distribution of incident x-rays is obtained using an unfolding method.

As the substrate of the segment detector, scintillators, semiconductors such as Si and CdTe can be used, according to the energy spectrum of x-rays to be measured and the x-ray absorption coefficient and the thickness of the substrate. In this paper, a commercially available CsI(Tl) scintillator array was employed for the convenience of proving the principle of the transXend detector.

2. Experiments

The experimental setup used to demonstrate the operation principle of the transXend detector is shown in **Fig. 2**. X-rays were emitted by an x-ray tube (TRIX-150S, Toreck, Co. Ltd., Japan). The voltages of the x-ray tube were 50, 65, and 80 kV. An aluminum filter (2 mm thick) was applied to reduce the low-energy x-rays. The x-rays passed through a lead collimator (5 mm thick, 5 mm hole diameter), a lanthanum (La) filter (100 μm thick), and an acryl phantom. The acryl phantom was 3 cm thick. It had 4 holes with the dimensions of 1 cm × 1 cm as water regions for thinned iodine tincture with different iodine thicknesses of 15, 30, 45, and 60 μm. Since the x-ray absorption by acryl is very similar to that of water, an acryl column was employed as a water region without iodine.

A CsI(Tl) scintillator array with photo diodes (S5668-11, Hamamatsu Photonics K. K., Japan) was used as the transXend detector. This array had 16 CsI(Tl) scintillators. The dimensions of each CsI(Tl) scintillator were 1.175 mm thickness, 2 mm width and 5 mm height. The space between the neighboring CsI(Tl) scintillators was 0.4 mm, which was stacked with TiO_2. The top and the side surfaces of the CsI(Tl) scintillators were also covered with TiO_2. For experiments, the first two scintillators were connected together and behaved as segment detector No. 1. In the same way, 12 scintillators were employed in total, which resulted in the 6-channel transXend detector.

Measurements were carried out by moving the acryl phantom along the *x*-axis shown in Fig. 2 with a precision stage (SGSP26-150, Sigma Koki Co., Ltd., Japan) with a 2.5 mm step. Output signals were amplified with a 6-channel current preamplifier (IPA-6, Raytech Corp., Japan), and read simultaneously using timer-counters with voltage-frequency converters (VFCT-8S4, Laboratory Equipments Corp., Japan). A computer with LabVIEW software controlled the precision stage and the timer-counters. A block diagram of the measurement system is shown in **Fig. 3**. A typical result of current measurements is shown in **Fig. 4** for the case of a 65 kV tube voltage.

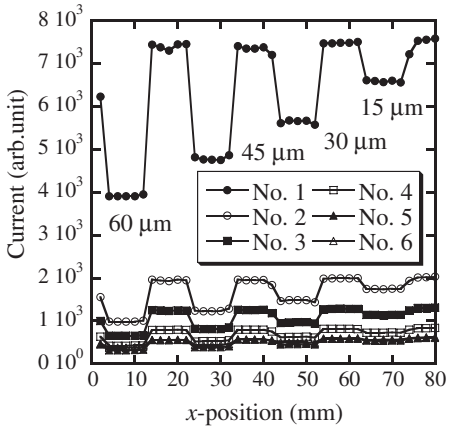

Fig. 4 Currents measured using a 6-channel CsI(Tl) transXend detector as a function of *x*-axis position. The four different iodine thicknesses in the acryl phantom are shown.

3. Unfolding Method

The calculated x-ray energy spectra after passing through the La filter (100 μm), water (acryl) layer (3 cm thick), and iodine (0, 30, and 60 μm) for the 65 kV tube voltage are shown in **Fig. 5**. As previously described,[1–4] the estimation of iodine thickness was performed using the x-ray events of two energy ranges: 28–33 and 34–39 keV. The purpose of unfolding measured currents is the estimation of x-ray events in these two energy ranges. Because all the x-rays injecting into the detectors contribute in the measured currents, we, however, defined six energy ranges for the unfolding process: E_1, 20–27 keV, E_2, 28–33 keV, E_3, 34–39 keV, E_4, 40–50 keV, E_5, 51–65 keV, and E_6, 66–80 keV.

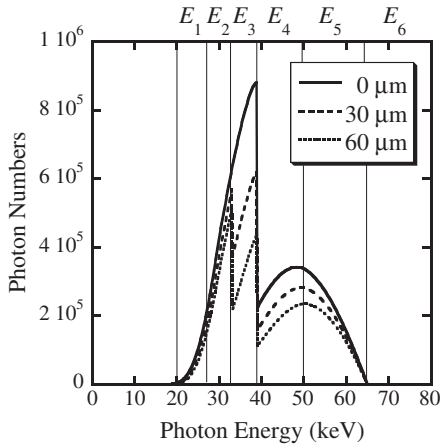

Fig. 5 Calculated x-ray energy spectra after passing the acryl phantom with iodine thicknesses of 0, 30, and 60 μm for the 65 kV x-ray tube voltage. Energy ranges, E_1 to E_6, were used in the unfolding processes.

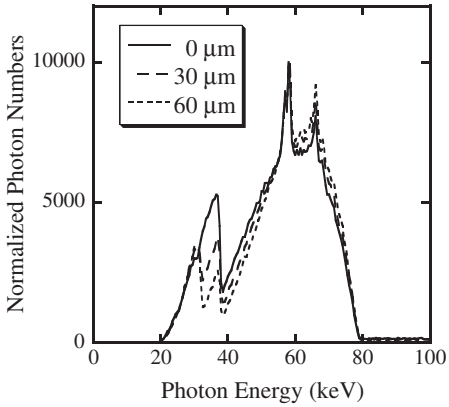

Fig. 6 X-ray energy spectra measured using a CdZnTe detector after passing the acryl phantom with iodine thicknesses of 0, 30, and 60 μm for the 80 kV x-ray tube voltage. Spectra are normalized at the maximum.

The relationship between the currents measured by the transXend detector and the x-ray energy distribution is written as

$$\begin{pmatrix} I_1 \\ I_2 \\ \cdot \\ \cdot \\ I_6 \end{pmatrix} = \begin{pmatrix} R_{11} & R_{12} & \cdot & \cdot & R_{16} \\ R_{21} & R_{22} & & & \cdot \\ \cdot & & \cdot & & \cdot \\ \cdot & & & \cdot & \cdot \\ R_{61} & \cdot & \cdot & \cdot & R_{66} \end{pmatrix} \begin{pmatrix} Y_1 \\ Y_2 \\ \cdot \\ \cdot \\ Y_6 \end{pmatrix}. \quad (1)$$

Here, I_i $(i = 1, 6)$ is the current measured at each segment detector of the CsI(Tl) transXend detector, and Y_j $(j = 1, 6)$ is the number of x-rays in the energy range E_j. The matrix R_{ij} $(i, j = 1, 6)$ is a response function. The response function contains the x-ray absorption rate as a function of x-ray energy, the position of a segment CsI(Tl) scintillator detector in the transXend detector, the rate of energy conversion to photons, the transmission efficiency of photons to the surface of the photo diode, and also the conversion efficiency of photons to electron-hole pairs in the photo diode.

With a simulation code such as EGS5,[5] deposited energies by incident x-rays could be calculated for each CsI(Tl) scintillator. However, the energy resolution of a scintillator does not accurately reflect the energy deposition in the output current; the process between the energy deposition and current production is very complicated, and the density and the photon reflection coefficient of TiO_2 painted on the surface of a CsI(Tl) scintillator were not described in the catalog of Hamamatsu Photonics K. K. Performing detailed experiments on the relationship between monochromatic x-ray absorption and output current was not practical. Furthermore, a simple calibration method must be established for the transXend detector for practical purposes. With these considerations, the response function was estimated first, using measured currents with iodine thicknesses of 0, 30, and 60 μm as references. With this response function, the currents measured for the phantom with iodine thicknesses of 0–60 μm were unfolded.

(1) Response Function

The estimation of the response function was performed for each x-ray tube voltage. The elements of the response function for the segment detector No. 1 of the CsI(Tl) transXend detector, R_{1j} $(j = 1, 6)$, are written as

$$\begin{pmatrix} I_{11} \\ I_{21} \\ \cdot \\ \cdot \\ I_{k1} \end{pmatrix} = \begin{pmatrix} Y_{11} & Y_{12} & \cdot & \cdot & Y_{16} \\ Y_{21} & Y_{22} & & & \cdot \\ \cdot & & \cdot & & \cdot \\ \cdot & & & \cdot & \cdot \\ Y_{k1} & \cdot & \cdot & \cdot & Y_{k6} \end{pmatrix} \begin{pmatrix} R_{11} \\ R_{12} \\ \cdot \\ \cdot \\ R_{16} \end{pmatrix}. \quad (2)$$

Here, I_{k1} is the current measured for the phantom with the iodine thickness k using the segment detector No. 1. The initial guesses of R_{1j} $(j = 1, 6)$ are calculated using mass absorption coefficients of CsI at each energy range.[6]

The x-ray energy distributions, Y_{kj} $(j = 1, 6)$, separated in the six energy ranges described above were obtained by calculations for the cases of x-ray tube voltages of 50 and 65 kV. The employed calculation code was based on the formula of Storm[7] and developed by the authors. The calculation results using the code showed good agreement with previous experimental studies.[1,2] For the case of the 80 kV tube voltage, the x-ray spectra obtained from experiments were used, as the characteristic x-rays emitted from the tungsten target were not accounted for in our calculation code. Typical measured x-ray spectra with the 80 kV tube voltage are shown in **Fig. 6**. X-ray energy measurements were performed using a CdZnTe detector (XR-100T-CZT, Amptek Inc., U.S.A.). The distortion of the spectra due to the escape of x-rays from the CdZnTe crystal was corrected via a stripping method.[8]

Unfolding was carried out using SAND II code,[9] which was performed to minimize the error S defined by the following equation,

$$S = \sum_{n=1}^{3} \left(I_{n1} - \sum_{j=1}^{6} Y_{nj} \cdot R_{1j} \right)^2. \quad (3)$$

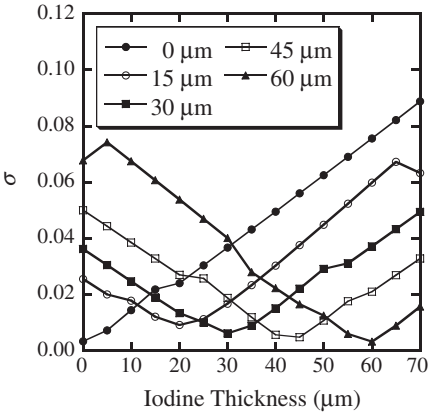

Fig. 7 σ, the differences of experiment-calculation results, obtained by the unfolding code SAND II for the case of the 65 kV x-ray tube voltage. The initial guess spectra were prepared by calculations with iodine thicknesses from 0–70 μm in 5 μm difference of iodine thickness. The iodine thickness of the initial guess spectrum with the minimum σ indicates the iodine thickness under survey. The iodine thicknesses employed in the experiments are shown.

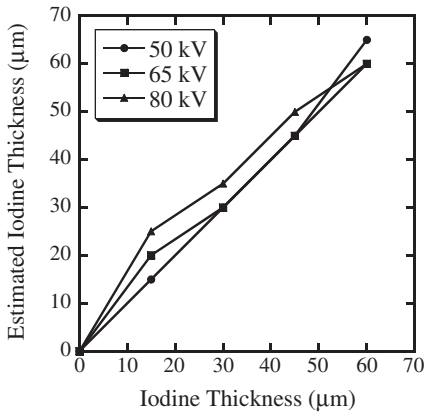

Fig. 8 Estimated iodine thickness obtained by the SAND II code with the minimum σ

Here, n represents the cases of iodine thicknesses of 0, 30, and 60 μm. In the same way, response functions for the segment detector from No. 2 to 6 were estimated.

(2) Unfolding

After the response function R_{ij} $(i, j = 1, 6)$ was obtained, Eq. (1) was unfolded for the measured currents. In the unfolding process, the calculated initial guess spectrum was changed for the ones with iodine thicknesses of 0–70 μm with the step of 5 μm for x-ray tube voltages of 50 and 65 kV. For the case of the 80 kV tube voltage, the initial guess spectra were obtained in experiments by changing the iodine thickness from 0–60 μm with the step of 5 μm, because the neat iodine tincture had 60 μm iodine thickness in 1 cm. By using the SAND II code, an initial guess spectrum among the data set of the initial guess spectra with different iodine thicknesses was found to have the minimum value of σ described using Eq. (4),

$$\sigma = \sqrt{\frac{1}{5}\sum_{i=1}^{6}\left(\frac{\sum_{j=1}^{6} R_{ij}Y_j}{I_i} - 1\right)^2}. \qquad (4)$$

Finally, the iodine thickness in the phantom was determined as the one that gave the initial guess spectrum in the simulation calculation for the cases of 50 and 65 kV tube voltages, and in the experiment for the 80 kV tube voltage.

III. Results and Discussion

The changes in σ as a function of the initial guess spectra with various iodine thicknesses for the 65 kV x-ray tube voltage are shown in **Fig. 7**. The estimated iodine thickness is the one of the initial guess spectrum, which gives the minimum σ for each measured current. The estimated iodine thickness is shown in **Fig. 8**. With the 50 kV x-ray tube voltage, the experimental result of 60 μm was overestimated as 65 μm. In the same way, the 15 μm experimental result with the 65 kV x-ray tube voltage and the 15–45 μm experimental results with the 80 kV x-ray tube voltage were overestimated to some extent. Because the unfolding process for the 80 kV x-ray tube voltage experiments was not performed for the initial guess spectra with iodine thicker than 60 μm, the agreement for the 60 μm iodine thickness was uncertain. Although the experimental results with iodine thicknesses of 0, 30, and 60 μm were employed to have response functions, the unfolded results for these iodine thicknesses were not always in agreement with the actual iodine thicknesses. However, in general, the estimation results were successful, with a nearly linear relationship between the actual and estimated iodine thicknesses. The accuracy of iodine thickness estimation by the unfolding method was inferior to the one obtained by the energy measurement of x-rays. The purpose of iodine thickness estimation is, however, for observing cancer tissue with iodine concentration higher than that in the normal tissue. Fluctuation in the estimated iodine thickness does not matter much in this application.

The obtained x-ray energy distributions for the tube voltages of 50, 65, and 80 kV are shown in **Figs. 9**, **10**, and **11**, respectively, as well as the input spectra for the cases of iodine thicknesses of (a) 15 and (b) 45 μm. The output spectrum of the unfolding code SAND II did not differ much from the input spectrum (Figs. 9–11). However, by using the minimum σ for the estimation as described above, the SAND II code gave near correct answers. From the energy distributions obtained for each iodine thickness, t, in the phantom, the event ratios $\{Y_3(t) - Y_2(t)\}/Y_2(t)$ are calculated and designated as $\Phi(t)$. Here, Y_2 and Y_3 are equal to ϕ_1 and ϕ_2 in previous papers.[1–4] With $\Phi(t)$, the iodine contrast $C(t)$ is estimated as

$$C(t) = \frac{\Phi(0) - \Phi(t)}{\Phi(0)}. \qquad (5)$$

The contrasts for each x-ray tube voltage as a function of the estimated iodine thickness can be seen in **Fig. 12**.

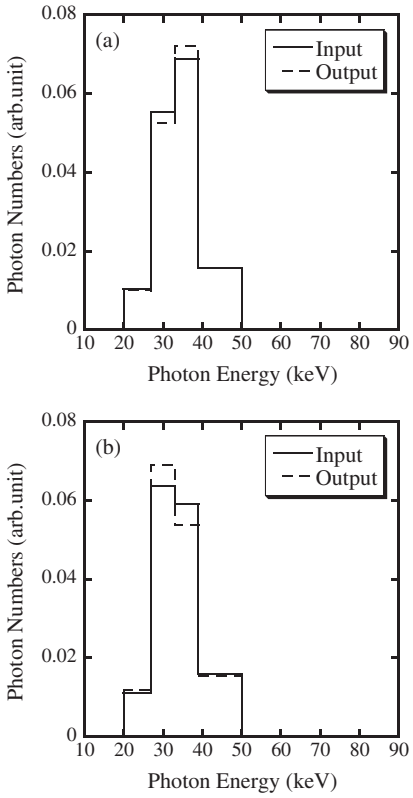

Fig. 9 Input and output spectra of SAND II code with iodine thicknesses of (a) 15 and (b) 45 μm for the case of the 50 kV x-ray tube voltage. The input and output spectra are normalized into unit area.

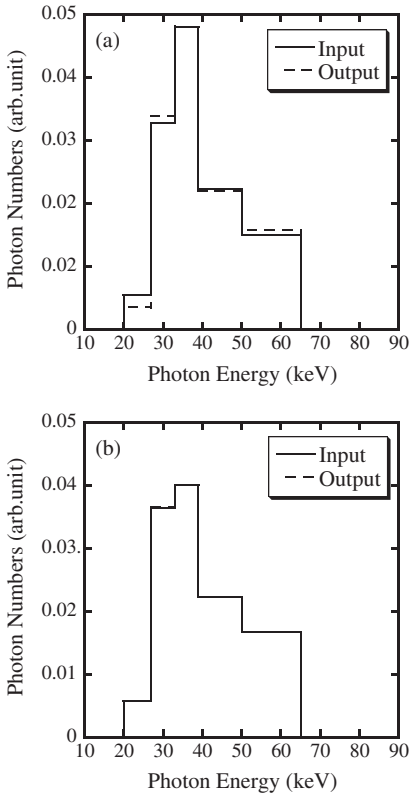

Fig. 10 The same with Fig. 9, but for the 65 kV x-ray tube voltage

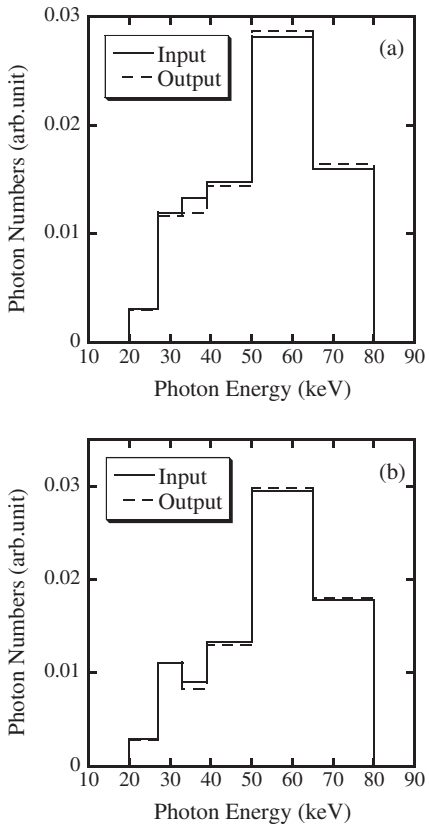

Fig. 11 The same with Fig. 9, but for the 80 kV x-ray tube voltage

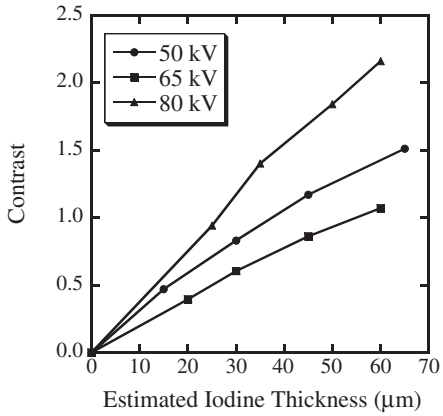

Fig. 12 Obtained iodine contrasts for the x-ray tube voltages of 50, 65, and 80 kV

By following the previous paper,[4] $Y_i(t)$ is written as

$$Y_i(t) = \Psi(E_i) \cdot \exp\{-\overline{\mu_I}(E_i) \cdot t\} \cdot \exp\{-\overline{\mu_W}(E_i) \cdot t_W\}. \quad (6)$$

Here, $\Psi(E_i)$ is the number of x-rays in the energy range E_i $(i = 2, 3)$ when there is no iodine and water, $\overline{\mu_I}(E_i)$ and $\overline{\mu_W}(E_i)$ are averaged absorption coefficients of iodine and water for the energy range E_i, and t_w is the thickness of water. With some calculations, the contrast is obtained as

$$C(t) = \frac{\{\overline{\mu_I}(E_3) - \overline{\mu_I}(E_2)\} \cdot t}{1 - \Psi(E_2)/\Psi(E_3) \cdot \exp[\{\overline{\mu_W}(E_3) - \overline{\mu_W}(E_2)\} \cdot t_W]}, \quad (7)$$

using Tayler expansion. The averaging of absorption coefficients must be done with the weighting of the x-ray spectrum. This causes the differences in the contrast as a function of x-ray tube voltage.

IV. Conclusions

We proposed a novel detector, termed the transXend detector, employing CsI(Tl) scintillators as the substrate, which gives the x-ray energy distribution when measuring x-rays as electrical currents. By using this detector, the unfolded iodine thicknesses were nearly proportional to the actual ones, and the obtained iodine contrasts were also proportional to the iodine thickness, which is encouraging considering that the energy resolution of CsI(Tl) scintillators is known to be not excellent.

The transXend detector concept should be useful for other applications requiring estimation of the energy distribution of x-rays and gamma rays under high photon flux. The choice of the detector substrate such as semiconductors, scintillators, or gas, and the thickness of the substrate enable the transXend detector to cope with the variety of x-ray energies. Mixtures of substrate materials and their thicknesses in one transXend detector might be useful for determining energy information for specialized purposes. Studies on the effects of changing the substrate material and the thickness of segment detectors on the performance of the transXend detector are in progress.

Acknowledgements

The authors wish to thank Dr. Y. Tomita, Hamamatsu Photonics, K. K., for the information on the CsI(Tl) scintillator array. This study was supported by a Grant-in-Aid for Scientific Research from the Japan Society for the Promotion of Science.

References

1) I. Kanno, S. Maetaki, H. Aoki, S. Nomiya, H. Onabe, "Low exposure x-ray transmission measurements for contrast media detection with filtered X-rays," *J. Nucl. Sci. Technol.*, **40**, 457 (2003).
2) I. Kanno, M. Takahashi, H. Aoki, H. Onabe, "Energy subtraction method with filtered x-rays for the detection of contrast media," *Nucl. Instrum. Methods Phys. Res.*, **A567**, 154 (2006).
3) I. Kanno, A. Uesaka, S. Nomiya, H. Onabe, "Comparison of current and energy x-ray measurement methods in contrast media detection," *Nucl. Instrum. Methods Phys. Res.*, **A580**, 534 (2007).
4) I. Kanno, A. Uesaka, S. Nomiya, H. Onabe, "Energy measurement of x-rays in computed tomography for detecting contrast media," *J. Nucl. Sci. Technol.*, **45**, 15 (2008).
5) H. Hirayama, Y. Namito, A. F. Bielajew, S. J. Wilderman, W. R. Nelson, "The EGS5 code system," SLAC-R-730 (2005) and KEK Report 2005-8 (2005).
6) E. B. Saloman, J. H. Hubbell, "X-ray attenuation coefficients (total cross sections): comparison of the experimental data base with the recommended values of Henke and the theoretical values of Scofield for energies between 0.1–100 keV," NBSIR 86-3431 (1986).
7) E. Storm, "Calculated bremsstrahlung spectra from thick tungsten targets," *Phys. Rev.*, **A5**, 2328 (1972).
8) M. Matsumoto, A. Yamamoto, I. Honda, A. Taniguchi, H. Kanamori, "Direct measurement of mammographic x-ray spectra using a CdZnTe detector," *Med. Phys.*, **27**, 1490 (2000).
9) W. McElroy, S. Berg, T. Crocket, G. Hawkins, "A computer-automated iterative method for neutron flux spectra determination for foil activation," AFWL-TR-67-41 (1967).